On long-baseline relative positioning with BDS-2/BDS-3/GPS data

Xiaoting Lei[1], Huizhong Zhu[1*], Jingfa Zhang[1] ,Jun Li[1] , Yangyang Lu[1]

1   School of Geomatics, Liaoning Technical University (LNTU), Fuxin 123000, China;

*   Correspondence: Huizhong Zhu, zhuhuizhong@lntu.edu.cn

Abstract: BeiDou global navigation satellite system (BDS-3) reached the global coverage in June 2020. To study the performance of the precise relative positioning using the BDS-3 alone and the improvement due to adding BDS-3 satellites to BDS-2 and GPS, this paper analysed the data of 033-039d provided by the MGEX in 2021. The fusion of BDS-2, BDS-3 and GPS data was conducted for static and dynamic high-precision long-baseline solution experiments. The influence of the individual BDS-2 / BDS-3 / GPS and by adding BDS-3 satellites to BDS-2 and GPS on precise relative positioning convergence speed and positioning accuracy were analyzed, respectively. The experimental results show that the current BDS-3 positioning performance (convergence speed and positioning accuracy) is similar to GPS, and the BDS-3 satellites effectively improve the positioning convergence speed upon BDS-2 and GPS. In the static positioning processing mode, with the aid of the BDS-3 satellites, the RMS (Root-Mean-Square) of the positioning errors using GPS only and the combination of BDS-2 and GPS was increased only by 20 % in the up direction, and for the BDS-2 system alone, the positioning accuracies in the E, N and U components were increased by 60%, 71% and 65%, respectively. In the dynamic positioning processing mode, after the addition of BDS-3 satellites, the positioning accuracies using GPS and GPS+BDS-2 in the E, N and U components were improved by about 15 %, 23 % and 23 %, respectively, and the BDS-2 positioning accuracies were improved by about 46 %, 38 % and 36 % in the E, N and U components, respectively.

1 Introduction

The Beidou Navigation Satellite System (BDS) is one of the Global Navigation Satellite Systems (GNSS), developed by China. By following the "three-step" strategic policy, China has steadily been promoting the development of the BDS. The BDS-1 was officially launched in 1994, and the BDS-2 system started in 2004 and was completed at the end of 2012 with the service for Asia-Pacific region [1]. BDS-3 has been developed since 2015 and put into a global service on July 31, 2020 [2]. The complete BDS-3 constellation consists of 24 Medium Earth Orbit (MEO) satellites, 3 Geostationary Earth Orbit (GEO) satellites and 3 Inclined Geo Synchronous Orbit (IGSO) satellites. In terms of its signals, BDS-3 satellites broadcast the B1I and B3I frequencies to achieve the compatibility with BDS-2. At the same time, in order to strengthen the compatibility and interoperability with other GNSS systems, BDS-3 has also been equipped with three new signals B2a, B2b and B1C [3], which can provide better positioning, navigation and timing (PNT) services for users globally [4].

Since the BDS was put into use, many scholars in China and abroad have done plenty of researches on its performance of BDS alone, or GPS + BDS combined [5-8]. Zhang et al. [9] show that the accuracy of a static baseline (medium baseline,

<100km) using the four-hour long BDS measurement data based on the broadcast ephemeris reached ±4cm. Pu et al and Wu et al. [10, 11] analyzed the relative positioning performance using the combination of the GPS, BDS and Galileo systems with the short baseline hybrid double-difference and short baseline single epoch tight combination. Their results showed that the dual-system or triple-system hybrid double-differencing technique can effectively accelerate the convergence speed toward the positioning accuracy improvement, and the tight combination model significantly improved the success rate and reliability in ambiguity fixing process. Jin et al. [12] showed that, in the solution of 5km short baseline, the accuracy through the combined BDS-2 and BDS-3 was improved in comparison with GPS or BDS-2 alone, at the positioning accuracy of within ±5mm.

To date, most researches have got involved in all aspects of BDS-2 positioning functions based on BDS-2, and mostly on precise relative positioning using BDS-2 alone or GPS + BDS-2 combined for short baselines. Therefore, this paper focuses on analyzing how significant the addition of BDS-3 satellites to each single GNSS, GPS and BDS-2 and the combined GPS+BDS-2 contributes to the performance of long-baseline solutions. Section 1 presents the mathematical model employed in this research, while Section 2 details the experiments of the chosen baselines of different lengths using the BDS-3 observation data and discusses the stability, convergence speed and positioning accuracy of the different GNSS constellations and their combinations in static and dynamic relative positioning from the results. Section 3 ends the manuscript with the conclusions and remarks. The outcomes from this research provide a valuable reference for the use of BDS-3 and its combined positioning with GPS.

2 Mathematical model and data processing strategy

2.1 Mathematical model

In this paper, the common frequencies of B1I, B3I from BDS-2 and BDS-3, and GPS L1 and L2 are used to form the double-differenced ionosphere-free combination to eliminate the influence of first-order error of the ionospheric delay. The equations of the original observables are:

$$P = \rho + H_k^j X + c \cdot dt_k - c \cdot dt^j + b_{r,k} - b_k^j - I_k^j + d_{trop} + \varepsilon_P \\ \Phi = \rho + H_k^j X + c \cdot dt_k - c \cdot dt^j + \lambda_j \left(B_{r,k} - B_k^j \right) - I_k^j + \lambda N_k^j + d_{trop} + \varepsilon_\Phi \right\} \tag{1}$$

where: P and Φ are the pseudo-range and carrier-phase measurements, respectively; ρ represents the geometric distance from a receiver station to a satellite; H is the linearized coefficient vector of the receiver's position, X is the 3D position correction vector of the receiver with respect to their approximations, k represents the receiver station; j represents the satellite ($j = 1, 2, …$); c is the speed of light in vacuum; dt_k is the receiver's clock error; dt_j is the satellite's clock error; $b_{r,k}$ and b_k^j represent the code hardware delays of the receiver and satellite, respectively; $B_{r,k}$ and B_k^j represent the phase hardware delays of the receiver and satellite, respectively; I is the ionosphere delay error; N is the carrier phase ambiguity with respect to the satellite; d_{trop} is the troposphere delay; ε_P、ε_Φ are other errors of pseudo-range and phase observations, including noise, multipath effect and so on. A pair of the observation equations as (1) could be made available for each of the visible satellites corresponding to each of a specific signal frequency, respectively. The equations of the double-differenced ionosphere-free combinations are:

$$\Delta\nabla P_{IF} = \Delta H_k^j X + \Delta\nabla\rho + \Delta\nabla d_{trop} + \Delta\nabla\varepsilon_P \\ \Delta\nabla\Phi_{IF} = \Delta H_k^j X + \Delta\nabla\rho + \lambda_{IF}\Delta\nabla N_{IF} + \Delta\nabla d_{trop} + \Delta\nabla\varepsilon_\Phi \right\} \tag{2}$$

where $\Delta\nabla$ represents the double-differencing

operator; the subscript *IF* represents the ionosphere-free combination, and the others are the same as in (1).

As well known, the zenith troposphere delay is divided into the dry and wet components. The dry component accounts for 80% - 90% of the total delay [16] and is corrected by using the Saatamoinen formulae, Then, the remaining wet component of tropospheric delay is estimated as follows:

$$d_{trop} = M_{dry}T_{dry} + M_{wet}T_{wet} \tag{3}$$

The ambiguity associated with a double-differenced ionosphere-free combination is expressed as:

$$\lambda_{IF}\Delta\nabla N_{IF} = \frac{f_1^2}{f_1^2 - f_2^2}\lambda_1\Delta\nabla N_1 - \frac{f_2^2}{f_1^2 - f_2^2}\lambda_2\Delta\nabla N_2 \tag{4}$$

$$\Delta\nabla N_{IF} = \frac{f_1}{f_1 - f_2}\Delta\nabla N_1 - \frac{f_1 f_2}{f_1^2 - f_2^2}\Delta\nabla N_{NW} \tag{5}$$

where $\Delta\nabla N_{NW} = \Delta\nabla N_1 - \Delta\nabla N_2$ is the wide-lane ambiguity, which can obtained by Melbourne-Wübbena (M-W) combination for inter epoch smoothing. The ambiguity $\Delta\nabla N_1$ in (5) has the integer characteristic and can be fixed by applying the Least-square AMBiguity Decorrelation Adjustment (LAMBDA).

1.2 Stochastic model

In general, the quality of the GNSS observation data and the elevation angles of the visible satellites are apparently related to each other. A consensus on the elevation angle of a satellite tells that the lower it is, the negative impact on the GNSS observations, the troposphere delay and multipath effect etc. would have [17]. This research specifically adopted the elevation angle based weighting model to determine the weight of corresponding observations:

$$\sigma^2 = \begin{cases} \dfrac{\sigma_0^2}{sin^2(E)}, E < 30° \\ \dfrac{\sigma_0^2}{sin(E)}, E \geq 30° \end{cases} \tag{6}$$

Moreover, the variances for pseudoranges and carrier phases are specified as follows:

$$D\left\{ \begin{pmatrix} \tilde{\Phi}_{IF} \\ P_{IF} \end{pmatrix} \right\} = \begin{pmatrix} \sigma_\Phi^2 & 0 \\ 0 & \sigma_P^2 \end{pmatrix} \tag{7}$$

wherein σ^2 means the variance of an observation; σ_0^2 is the a priori variance factor; E is the elevation angle of a satellite; $D\{\bullet\}$ represents the variance (matrix) operator; σ_φ^2 and σ_P^2 represent the variances of a pseudorange and a carrier phase observation, respectively..

2 Experiments and their analysis

The stations, YAR2 and NNOR in Australia and TASH, KITG, KIT3, USUD and MIZU in Asia provided by the Multi-GNSS Experiment (MGEX) observation network were chosen for our experiments in this research (Figure 1). By using the seven-day observation data from 033d to 039d in 2021, four baselines, KITG-KIT3 (190 m), YAR2-NNOR (236 km), TASH-KITG (318 km) and USUD-MIZU (413km) were formed. An overview of the formed baselines is given in Table 1. The station coordinates in the Solution INdependent EXchange Format (SINEX) weekly solution file released by the international GNSS service (IGS) were taken as their true coordinates, whilst the phase center offsets (PCO) and phase center variation (PCV) corrections of GPS satellites and receiver antennas were taken from the ANTEX file issued by IGS. However, the current international service center only provides the BDS satellite PCO correction [18]. The positioning performance of the different GNSS systems was analyzed in terms of the convergence speed and positioning accuracy with the BDS-2, BDS-3 and GPS individually and their varied combinations, which are specified in the context of the individual tests.

In data processing, the cut off elevation angle was set to 7° and the used sample interval of the observation data was 30s. The precise orbital products provided by the German Research Center for Geosciences (GFZ) were used. The troposphere delays were corrected by the Saatamoinen model and their residual errors were modeled, whilst the first-order ionosphere delay was eliminated by

applying the ionosphere-free combination. The least-square method was implemented for baseline estimation. The LAMBDA algorithm was used to fix the ambiguity parameters. The systematic errors such as the phase winding up, Earth's rotation, relativistic effect and solid tide were corrected by the commonly available models accordingly. A summary of data processing strategy is given in Table 2.
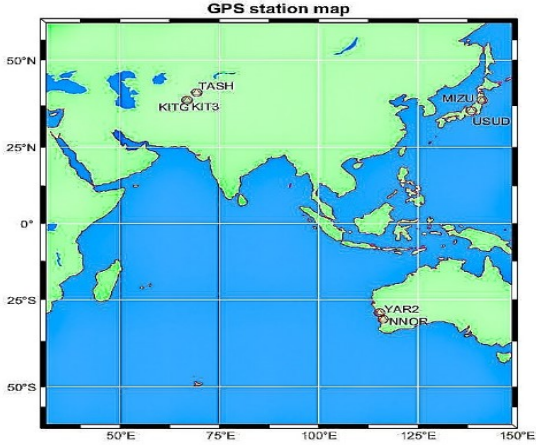
Figure 1: Distribution of stations

2.1 Data quality analysis

To ensure the data availability in the experiments before the data processing, the data quality is analyzed in three aspects: the satellite visibility, signal-to-noise ratio and multipath error effect. By taking the data on the DOY of 033 in 2021 as an example, it can be seen from Figure 2 that the number of the common visible BDS-3 satellites was more than that of the BDS-2 satellites, and the number of the common visible BDS-3 satellites was between 6 and 11. Specifically, the number of the common visible BDS-3 satellites for the baseline of USUD-MIZU (413km) in Asia was 9, and the number of the common visible BDS-2 satellites was about 8. With GPS, the number of the common visible satellites between stations maintained between 6 and 12. The number of the common visible GPS satellites for the baselines of KITG-KIT3 (190 m) and DASH-KITG (318 km) was significantly more than the one of the common visible BDS satellites, which was about 9 to 10 satellites. In general, The numbers of the common visible satellites from

BDS-2, BDS-3 and GPS were sufficient for conducting our experiments.

Table 1: Baseline information

length	station	longitude	latitude	Antenna type	
190 m	YAR2	115°E	29°S	AOAD/M_T	NONE
	NNOR	116°E	31°S	SEPCHOKE B3E6	NONE
236 km	TASH	69°E	41°N	SEPCHOKE B3E6	NONE
	KITG	66°E	39°N	TRM59800.00	SCIS
318 km	USUD	138°E	36°N	AOAD/M_T	JPLA
	MIZU	141°E	39°N	SEPCHOKE B3E6	NONE
413 km	KITG	66°E	39°N	TRM59800.00	SCIS
	KIT3	66°E	39°N	SEPCHOKE_B3E6	NONE

Table 2: Data processing strategy

DOY (observation data)	033d - 039d, 2021
Positioning mode	Precise relative positioning
Satellite systems	BDS-2、BDS-3、GPS
Satellite orbital products	Precise products provided by GFZ
Cut off elevation angle	7°
Sample interval	30 seconds
Troposphere dry delay	Saastamoinen
Troposphere wet delay	Estimated as parameters
Ionosphere	Ionosphere-free combination
Estimation method	Least-square
Ambiguity fixing method	LAMBDA

The average values of Signal-to-Noise Ratio (SNR) and multipath error in the data at each station during 7 days from 033d to 039d were analysed and presented in Figure 3 and Figure 4, respectively. The SNR, the ratio of signal strength of carrier observation to noise strength [19], can be used to measure the quality of the acquired satellite signals and the unit in dB-Hz. The higher the SNR, the higher data quality the carrier phases would have. As can be seen from Figure 3, the SNR of B3I was the highest. L1 and B1I were similar which maintained above 40 dB−Hz. The SNR of the L2 signal was low, but still higher than the minimum threshold of 30 dB−Hz required by a standard data processing.
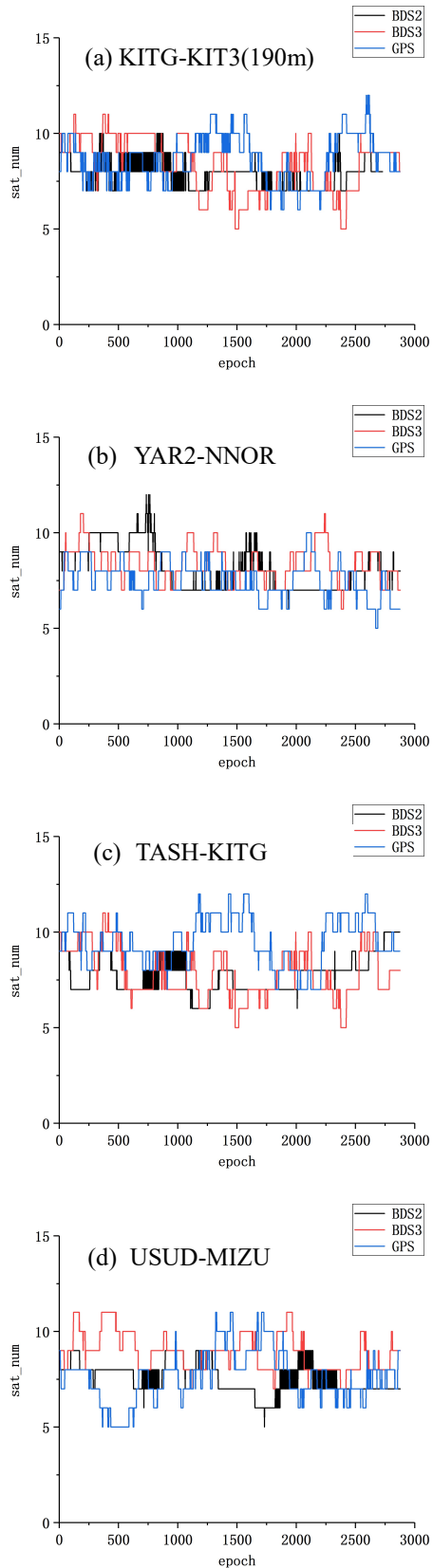
Figure 2: Total Number of common visible

Satellites among Stations
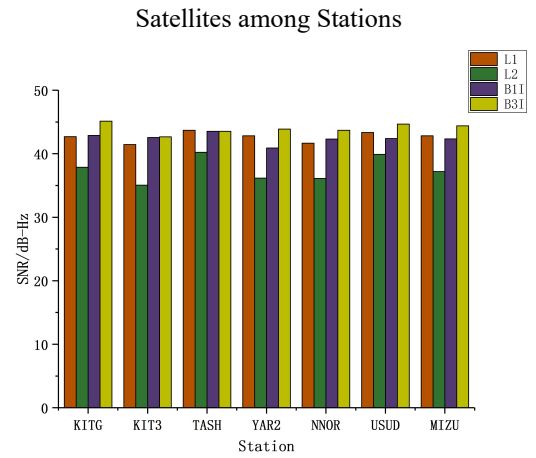
Figure 3: Signal-Noise Ratio of Each Station
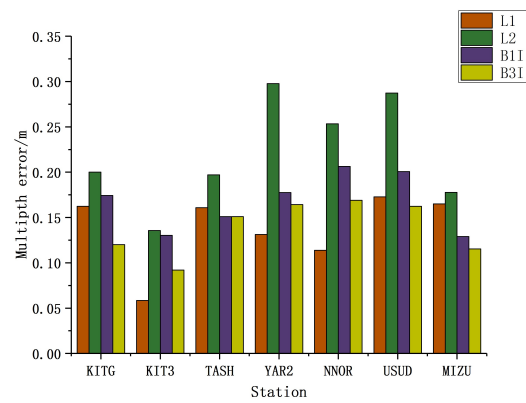
Figure 4: Multipath Error on Signals at Each Station

In the process of signal propagation, the acquired satellite signal could be affected by the observation environment. For example, a receiver may receive the excess reflected signal from a certain type of the signal reflections, which is called multipath error. In comparison with the phase observations, the multipath error on pseudo-ranges could be large, even reach 0.5 code element width [20]. Figure 4 presents the multipath errors from four signals, of which the GPS L2 signal suffered from the largest multipath error, the multipath errors on BDS B1I were larger than that on B2I, whilst the GPS L1 signal had the best suppression of the multipath errors and possessed the best observation quality. In general, the multipath error in pseudo-ranges at each station signal was within 0.3 m.

2.2 Convergence speed

139

The commonly used evaluation measure is the convergence speed, which statistically analyses the convergence time, i.e., the Time To First Fix (TTFF). In order to introduce the TTFF analysis, with the 7-day data from 033d to 039d in 2021, the 24-hour daily data were divided into the 6-hour long sub-periods. The starting hour of each sub-period is one hour shifted from its previous one, which are 00:00:00, 01:00:00,..., Respectively (e.g., 00:00:00-06:00:00, 01:00:00-07:00:00…). In the static and dynamic positioning processing mode, seven different combinations of GPS, BDS-2 and BDS-3 are solved, and the baseline vector (i.e., the ECEF incremental coordinates) between two stations need to be converted into their E, N, and U components relative to the base station. To ensure a reliable statistics, the differences in E, N, U directions of 20 consecutive epochs after the convergence time needs to reach and maintain their magnitudes relative to their references at the centimeter level. Hereupon, the statistics of the convergence time with the different combinations within each sub-period of the four groups of baselines was carried out respectively, and then the dynamic and static convergence rates associated with the seven combinations were analyzed. The statistical results are shown in Table 3 and Table 4, respectively while the convergence time statistics of static and dynamic solutions are shown in Figure 5 and Figure 6, respectively.

In the static positioning processing mode, as shown in Table 3, the convergence process of resolving the short baseline is faster than the one of resolving the long baseline. The average convergence time with GPS alone remained within 20 min. Due to the sufficient number of common visible GPS satellites observed over the baseline of TASH-KITG (318 km) in Asia, the convergence speed was the fastest, reaching the centimeter accuracy in about 6 minutes. The number of the observed BDS-3 satellites in Asia was large, and its convergence speed was equivalent to or even better than with GPS. The average convergence time of GPS+BDS-3 dual-system was within 10 min, 63% higher than that of GPS alone. The convergence speed of BDS-2

alone was the slowest with the average convergence time of nearly 50 min. The average convergence time of BDS-2+ BDS-3 dual-system remained about 15 min, about 70% higher than that of BDS -2 only. As can be seen from Figure 5, the worst convergence process happened to BDS-2 only on the DOY of 034d in 2021 for 58 min. With the aid of BDS-3 satellites, the convergence time was decreased down to 9 min, and the convergence speed was increased by 84%. The improvement of the convergence process of GPS+BDS-2 dual-system was good, which reached the centimeter accuracy in about 10 minutes. Furthermore, the overall convergence speed was increased by about 40% after having integrated the BDS-3 satellites.

In the dynamic positioning processing mode, the baseline results are summarized in Table 4. The convergence time of GPS only was about 50 min. By adding BDS-3 satellites, the convergence time was decreased down to about 20 min, an incensement of the convergence speed by about 60%. The convergence speed of BDS-3 only was the same as that of GPS, which maintained to be about 50 min, as the convergence speed of BDS-2 only was the slowest in dynamic mode. As can be seen from Figure 6, the convergence speed of BDS-2 only was consistent in various regions and the average convergence time was about 140 min. With the aid of the BDS-3 satellites, it took about 30 min to achieve cm level convergence accuracy, and the overall convergence speed was increased by 80%. From the combined GPS+BDS-2, the convergence time was stably about 30 minutes. The addition of the BDS-3 satellites decreased the convergence time down to 15 minutes, i.e., a 50% improvement.

In general, the BDS-2 positioning process in static and dynamic modes went convergent significantly slower than GPS. Although the number of the BDS-2 satellites at most of epochs was not less than the number of the GPS satellites, the number of the BDS-2 MEO satellites was low, and the orbit accuracy of the BDS-2 satellites was lower than that of the GPS satellites. So, the BDS-2 convergence time was much longer than GPS. Many more MEO

satellites have been launched with the BDS-3 system, and their orbit accuracy has been better than that of

(a) KITG-KIT3(190m)

(b)YAR2-NNOR(236 km)

(c) TASH-KITG(318 km)

(d) USUD-MIZU(413 km)
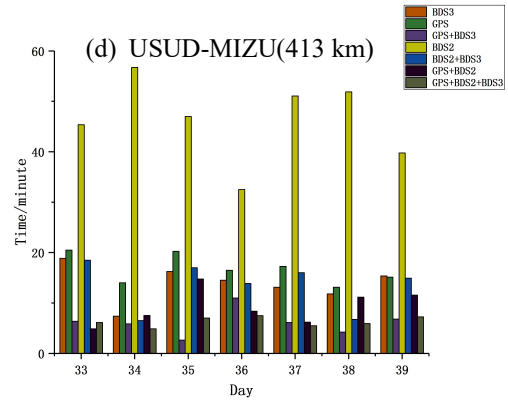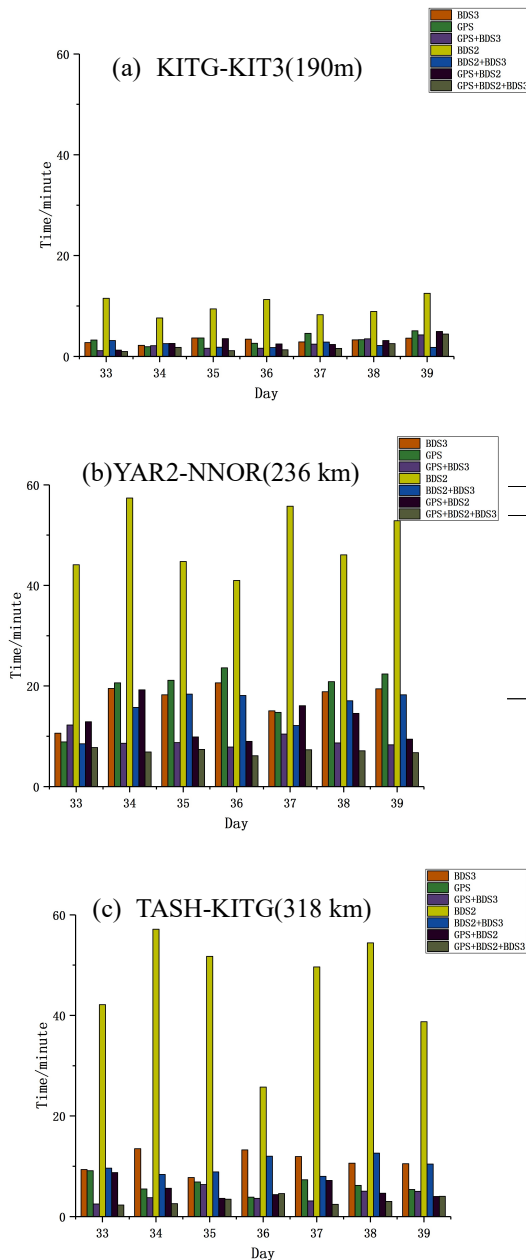
Figure 5: Static Mode Convergence Time Statistics

Table 3: Statistics of Mean Convergence Time of Static Mode (min)

TYPE	190 m	236 KM	318 KM	413 KM
BDS-3	3.12	17.78	11	13.9
GPS	3.49	18.89	6.32	16.68
GPS+BDS-3	2.39	9.28	4.21	6.16
BDS-2	9.95	48.84	45.65	45.33
BDS-2+BDS-3	2.29	15.46	9.99	13.37
GPS+BDS-2	2.9	13.01	5.46	9.21
GPS+BDS-2+BDS-3	1.97	7.04	3.2	6.31

Table 4: Statistics of mean convergence time for dynamic models (min)

TYPE	190 m	236 km	318 km	413 km
BDS-3	18.82	51.89	51.24	51.41
GPS	20.76	47.93	48.79	55.29
GPS+BDS-3	12.07	23.42	20.16	17.23
BDS-2	53.74	141.64	136.36	138.9
BDS-2+BDS-3	16.18	33.86	32.22	25.58
GPS+BDS-2	17.74	33.66	26.54	27.19
GPS+BDS-2+BDS-3	10.32	17.82	15.79	15.09

BDS-2 satellites. The BDS-3 convergence speed has been better than BDS-2 and became equivalent to GPS.

With the addition of BDS-3 satellites to the GPS+BDS-2 combined system, the convergence speed has been increased by about 30% in both static and dynamic modes. The convergence speed of the GPS positioning solution reached about 60% improvement with the aid of the BDS-3 satellites. The BDS-2 only solution convergence speed was slow. However the addition of the BDS-3 satellites to the BDS-2 improved the convergence speed by about

70-80%, which significantly reduced the BDS-2's convergence time. The BDS system (BDS-2+BDS-3) functioned better than that of GPS only in terms of the positioning convergence speed.

(a)KITG-KIT3(190m)

(b) YAR2-NNOR(236 km)

(c) TASH-KITG(318 km)

(d)USUD-MIZU(413 km)
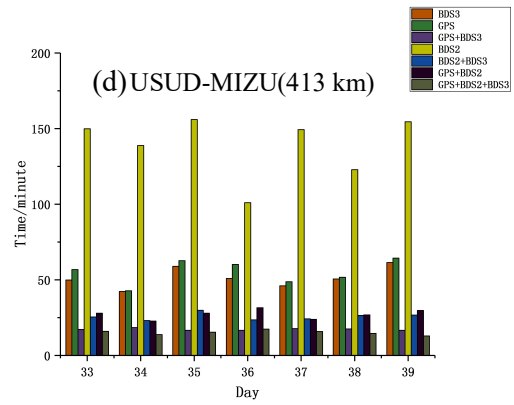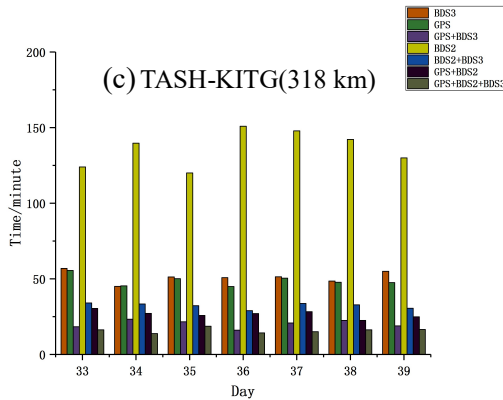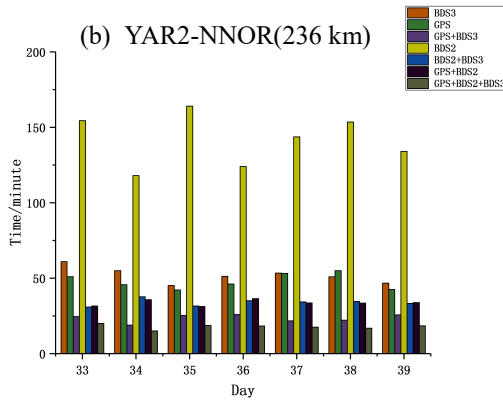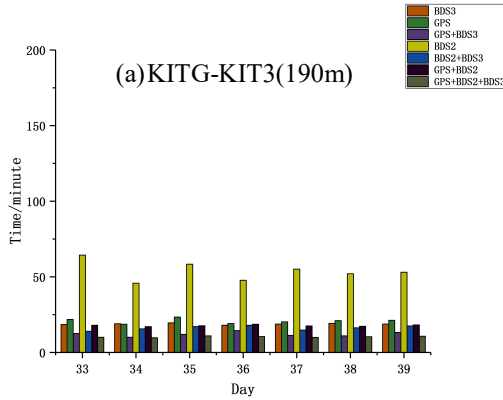
Figure 6: Dynamic Model Convergence Time Statistics

2.3 Positioning accuracy

This sub-section mainly analyzed how the addition of the BDS-3 satellites improves the positioning accuracy in different positioning modes by overviewing the solutions of each sub-period with the data from 33d-39d in 2021. In the static mode, the resulted differences of the E, N and U components at the last epoch of each sub-period were taken as the final positioning deviations. The average values of all the differences were considered as the static positioning errors. The results are given in Table 5 whilst the detailed positioning deviations of each station from the DOY 033d to the DOY 039d is shown in Figure 7. In the dynamic mode, by taking the results from the remaining epochs after the convergence was reached during each sub-period, the RMS in E, N and U were calculated, and the average values of RMS of all data deviation sequences were considered as the dynamic positioning results (shown in Table 6). The detailed positioning deviations of each station on each day are shown in Figure 9.

142

(a) KITG-KIT3(190 m)

(c) TASH-KITG(318 km)

(b) YAR2-NNOR(236 km)

(d) USUD-MIZU(413 km)
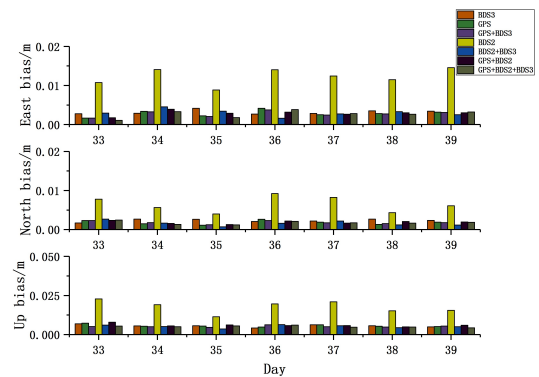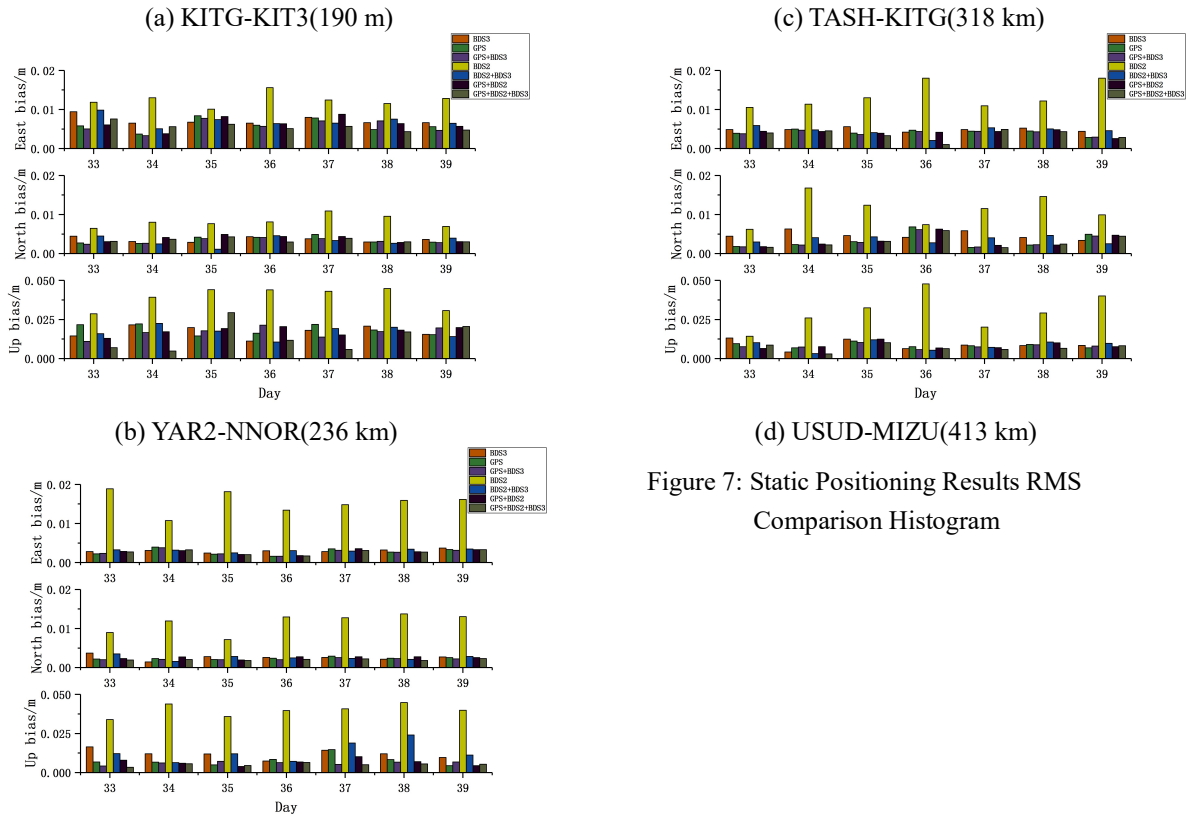
Figure 7: Static Positioning Results RMS
Comparison Histogram

Table 5: Seven Day Average RMS Statistics of Static Positioning Results (cm)

TYPE	190 m			236 km			318 km			413 km		
	E	N	U	E	N	U	E	N	U	E	N	U
BDS-3	0.32	0.23	0.56	0.72	0.36	1.73	0.3	0.26	1.19	0.46	0.47	0.88
GPS	0.28	0.18	0.56	0.6	0.35	1.85	0.28	0.24	0.77	0.41	0.32	0.85
GPS+BDS-3	0.27	0.18	0.51	0.58	0.32	1.68	0.27	0.22	0.61	0.4	0.3	0.79
BDS-2	1.2	0.65	1.8	1.24	0.82	3.92	1.54	1.15	3.98	1.34	1.12	2.99
BDS-2+BDS-3	0.3	0.16	0.51	0.7	0.32	1.71	0.31	0.25	1.31	0.45	0.36	0.83
GPS+BDS-2	0.29	0.18	0.6	0.61	0.37	1.76	0.28	0.23	0.66	0.41	0.32	0.83
GPS+BDS-2+BDS-3	0.26	0.17	0.51	0.57	0.34	1.38	0.27	0.2	0.51	0.39	0.3	0.69

In the static positioning processing mode, as can be seen from Table 5, the long-baseline static relative positioning horizontal accuracy using GPS plus BDS-3 in each region was approximately the same as using GPS only., however, the vertical accuracy was improved to a certain extent. Specifically with the TASH-KITG (318) baseline in Asia , the GPS RMS of positioning differences in the E, N and U directions were 0.28 cm, 0.24 cm and 0.77 cm, respectively. With BDS-3 satellites together, the RMS in the E, N and U directions were about 0.27, 0.22 and 0.61 cm. The horizontal accuracies in the E and N directions were similar to the ones from GPS only solution, but the accuracy in the vertical direction

was increased by about 20%. It can be seen from Figure 7 that the positioning accuracy of the BDS-3 only is slightly lower than that of the GPS only. The BDS-2 only performance was poor in comparison with the BDS-3 and GPS individually, but the combined BDS-2 and BDS-3 significantly improved the positioning accuracy. The most significant accuracy improvement was with the baseline of TASH-KITG (318) in Asia. Specifically, the positioning accuracy in E, N and U directions were increased to 0.31 cm, 0.25 cm and 1.31 cm from 1.54 1.15 cm and 3.98 cm, respectively, , which presented the positioning accuracy improvement by 80% (East), 78% (North) and 67% (Up), respectively. With GPS,

143

BDS-2, and BDS-3 together, although the positioning accuracy remained quite the same horizontally as without using the BDS-3 satellites and only 20% improvement vertically, the positioning reliability and measurement availability have been clearly improved.

In order to more specifically compare the influential effect of the addition of the BDS-3 satellites to BDS-2, BDS-2 and BDS-2+BDS-3 are analyzed in detail, taking DOY 34d in 2021 as an example(The data segmentation method is the same as that in Section 2.2). As can be seen from figure 8, adding the BDS-3 satellites has significantly improved the positioning performance upon of the BDS-2, which reached a horizontal accuracy at the millimeter level, specifically by about 60%, 71% and
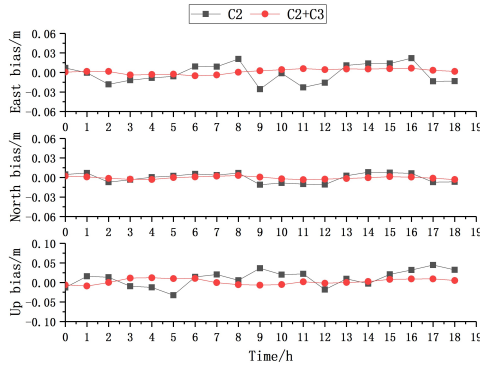
（a）KITG-KIT3(190 m)
（b）YAR2-NNOR(236 km)
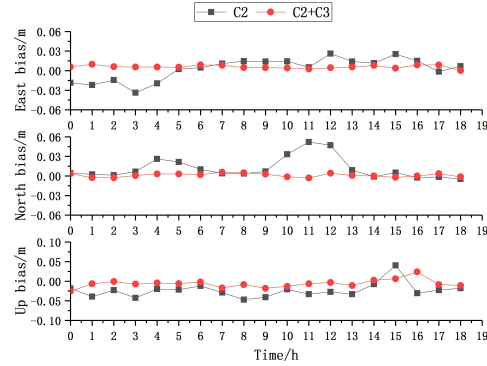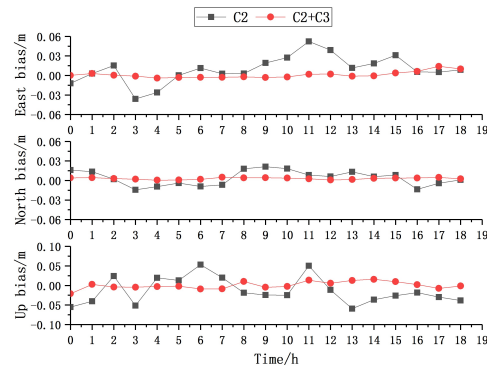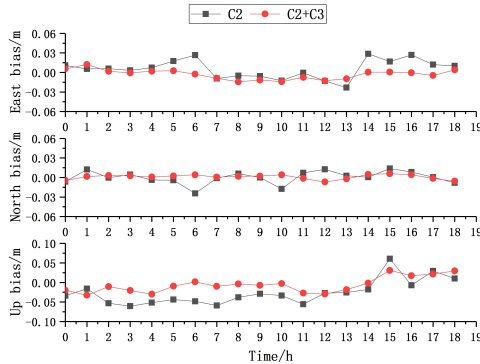
（c）TASH-KITG(318 km)
（d）USUD-MIZU(413 km)

Figure 8: Static Positioning Results of BDS-2 and BDS-2+BDS-3

65% (the RMS from 1.49, 1.0 and 3.27 cm to 0.59, 0.29 and 1.14 cm) in three directions (E, N, Up). This is similar to GPS.

In the dynamic positioning processing mode, it can be seen from Figure 9 that in the four sets of baselines, GPS and BDS-2 single system and GPS+BDS-2 dual-system have different degrees of improvement in E, N and U directions after adding BDS-3 satellites. The average RMS of positioning differences in the E, N and U directions of single GPS is 1.84 cm, 1.4 cm and 3.15 cm respectively. After adding BDS-3 satellites to form GPS+BDS-3 dual-system, the average RMS in three directions is 1.59 cm, 1.1 cm and 2.5 cm respectively, which increased by about 14%, 21% and 21%. The BDS-2 and BDS-3 single system compared to GPS single system, The following conclusions can be obtained that the GPS positioning accuracy is optimal and BDS-3 positioning accuracies is slightly lower than GPS but better than BDS-2. The BDS-2 maximum differences are close to 4 cm in the E direction and 6

cm in the U direction, respectively. With the aid of BDS-3 satellites, BDS-2 RMS values are decreased from 3.26 cm, 2.53 cm and 5.13 cm to 1.75 cm, 1.56 cm and 3.29 cm in E, N and U, respectively, i.e., their accuracies are increased by 46%, 38% and 36%, correspondingly. Compared with GPS, the dynamic relative positioning performance with the BDS-2+BDS-3 dual-system is better. After having added the BDS-3 satellites to the GPS+BDS-2 dual-system, the dynamic and the static positioning mode are improved in the E, N and U directions. The average RMS increases from 1.74 cm, 1.28 cm and 2.94 cm to 1.47 cm, 0.96 cm and 2.24 cm, which promoted about 16%, 25% and 24%, respectively.

To more intuitively study the impact of adding BDS-3 on positioning, in the dynamic positioning processing mode, using the data of DOY 34d in 2021 and the dynamic positioning performance is analyzed by seven different combinations(BDS-2, BDS-3, GPS, GPS + BDS-3, BDS-2 + BDS-3, GPS + BDS-2, GPS + BDS-2 + BDS-3).
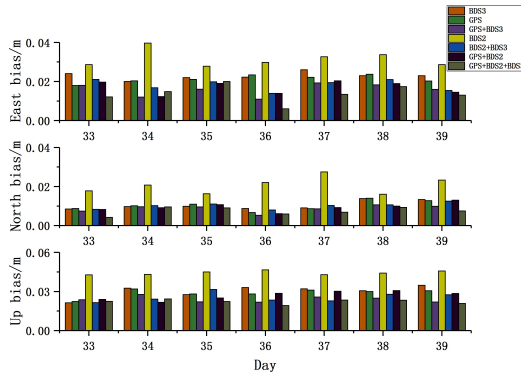
(b) YAR2-NNOR(236 km)

(c) TASH-KITG(318 km)

（a）KITG-KIT3(190 m)
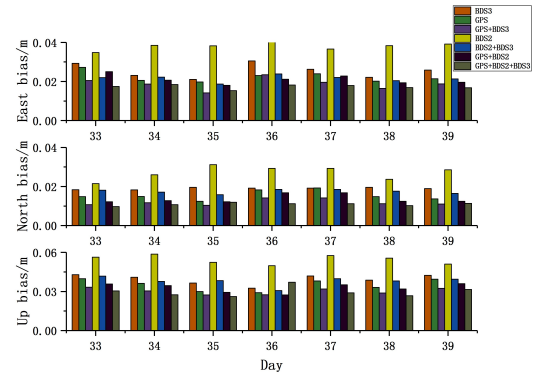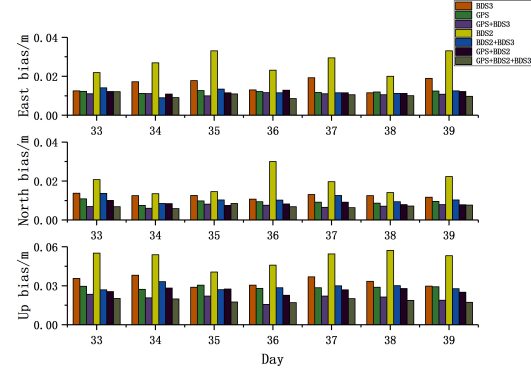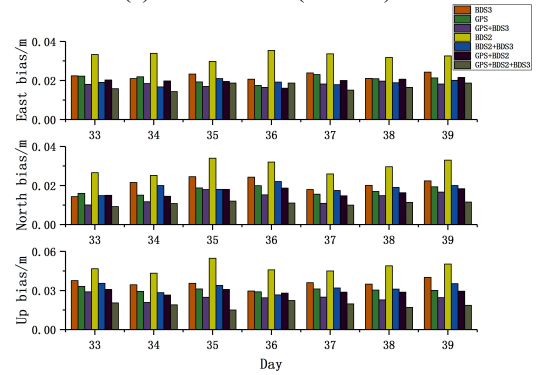
(d) USUD-MIZU(413 km)

Figure 9: Dynamic Positioning Results RMS Comparison Histogram

Table 6: Seven Day Average RMS Statistics Result of Dynamic Positioning Mode (cm)

TYPE	190 m			236 km			318 km			413 km		
	E	N	U	E	N	U	E	N	U	E	N	U
BDS-3	2.29	1.04	3.03	2.55	1.9	3.94	1.57	1.24	3.33	2.24	2.07	3.54
GPS	2.12	1.02	2.89	2.23	1.54	3.51	1.21	0.93	2.88	2.09	1.73	3.06
GPS+BDS-3	1.57	0.87	2.39	1.88	1.19	3.02	1.09	0.71	2.05	1.8	1.39	2.44
BDS-2	3.16	2.05	4.43	3.8	2.71	5.45	2.68	1.93	5.15	3.3	2.95	4.78
BDS-2+BDS-3	1.82	1.01	2.56	2.15	1.74	3.8	1.19	1.07	2.9	1.9	1.88	3.18
GPS+BDS-2	1.69	0.95	2.69	2.09	1.36	3.29	1.18	0.84	2.62	1.96	1.65	2.9
GPS+BDS-2+BDS-3	1.38	0.75	2.22	1.73	1.09	2.98	1.01	0.7	1.86	1.68	1.09	1.89

The GPS+BDS-3 combination possessed the best and most stable solution, as the BDS-2 only solution was the worst, partially with the large fluctuation. The combination of the BDS-3 and BDS-2 speeded up the solution convergence. Besides, the positioning accuracy also received a better lifting effect. By taking the baseline of USUD-MIZU (413 km) in Asia as an example, the number of the observed BDS-2 satellites was relatively low during the 12-16 h on that day so that the result can't go convergent during dynamic data processing. However, after having included the BDS-3 satellites, the solution accuracy was effectively improved down to centimeter-level. The combined BDS-3+GPS and BDS-3+GPS+BDS-2 have also improved the solution accuracy in all of the three directions. It can be seen from Figure 10 that the data will jump in the last 15 minutes of each day, which is due to the influence of the daily boundary discontinuities (DBD) [21,22].

3 Conclusion

Based on the observation data provided by MGEX and the precise products released by GFZ, this research conducted specific experiments on the long baseline relative positioning in static and dynamic modes using BDS-2, BDS-3 and GPS individually and different combinations of them and obtained the following conclusions through the comparative analysis in terms of data quality, convergence speed and positioning accuracy:

(1) In the static and dynamic data processing modes, the convergence speed and positioning accuracy using BDS-3 are similar to GPS, and the positioning accuracy meets the requirements of current high-precision positioning;

(2) The inclusion of the BDS-3 satellites in addition to GPS, BDS-2 and GPS+BDS-2 in precise relative positioning can effectively improve the solution convergence speed, especially for BDS-2;

(3) In the static precise relative positioning mode, the addition of the BDS-3 satellites to GPS, and GPS+BDS-2does not significantly improve the horizontal positioning accuracy, but the vertical accuracy by about 20%. The formation of BDS-2+BDS-3 has increased the accuracy in the E, N and U directions by about 60%, 71% and 65% respectively. The accuracy in E and N directions maintained within 1 cm while the accuracy in the U direction was kept within 2 cm;

(4) In the dynamic precise relative positioning mode, The inclusion of the BDS-3 satellites in GPS and in GPS+BDS-2 has made a consistent improvement. The positioning accuracy in the E, N and U directions has been improved by about 15%, 23% and 23%, respectively. The positioning accuracy with using BDS-2+BDS-3 has been improved by about 46%, 38% and 36% in E, N and U directions, respectively.

（a）TASH-KITG(318 km)　　　　　　　　（b）USUD-MIZU(413 km)
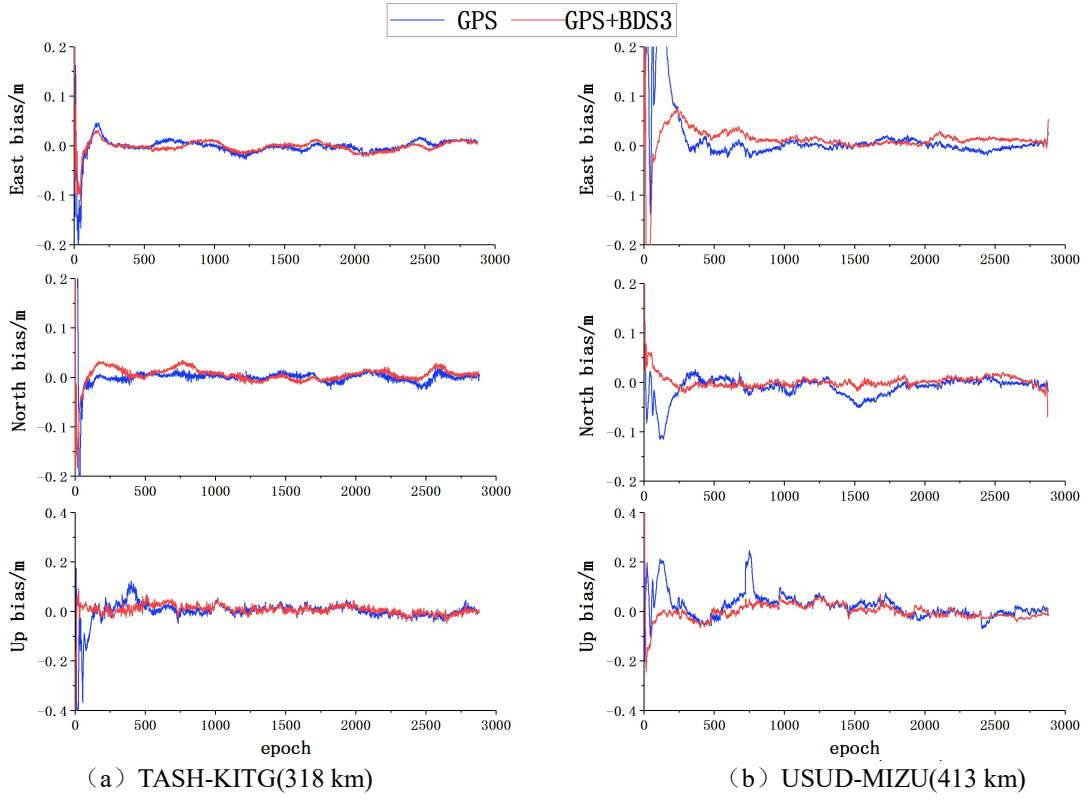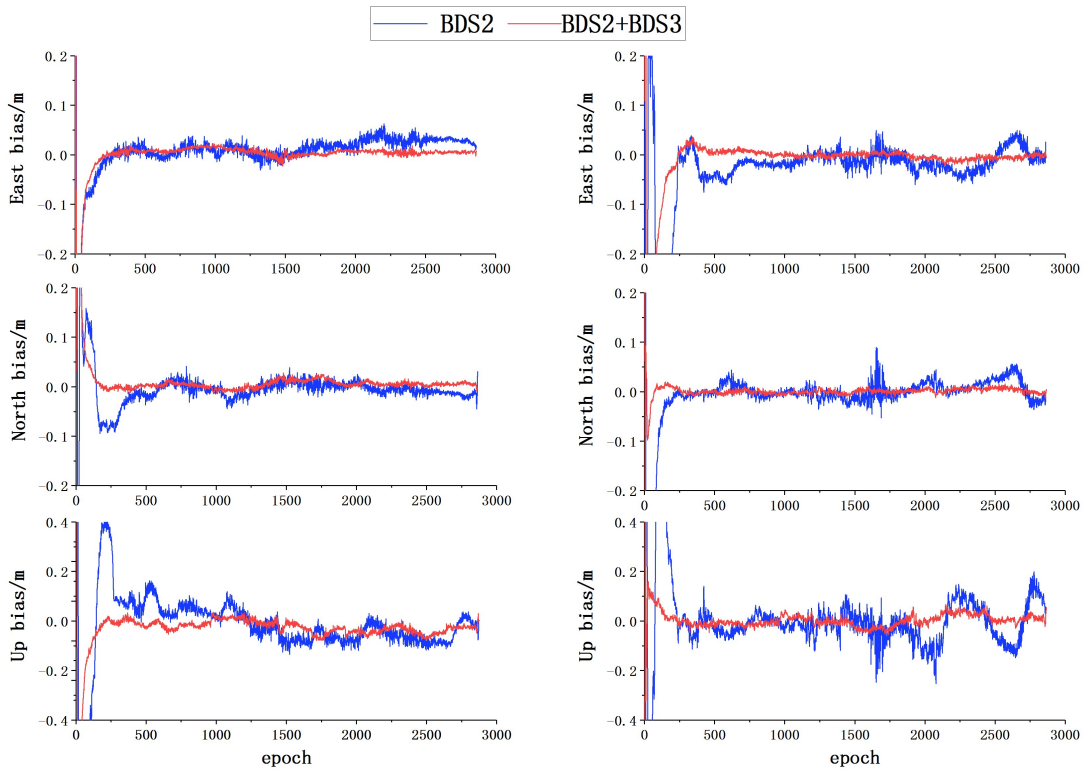
（c）TASH-KITG(318 km)　　　　（d）USUD-MIZU(413 km)
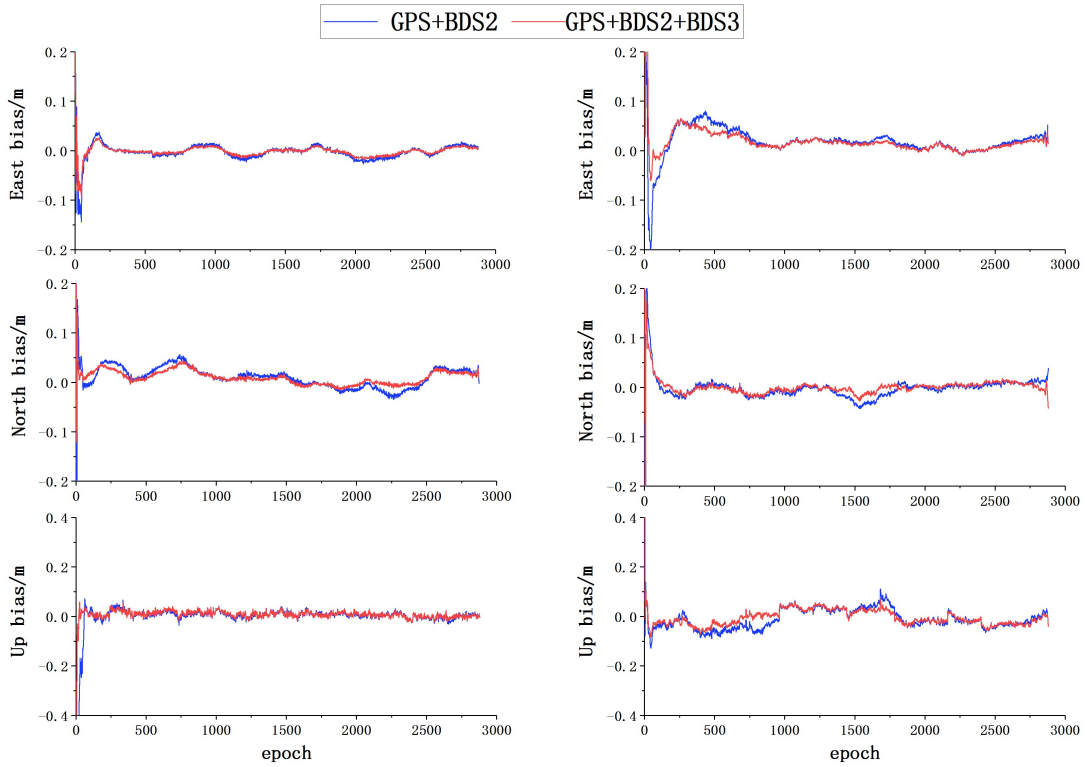
（e）TASH-KITG(318 km)　　　　（f）USUD-MIZU(413 km)

Figure 10: All-day Dynamic Mode Positioning Deviation Statistics with 24 h

References

[1] Development Report of the Beidou Satellite Navigation System [J]. International Space, 2012(04):6-11.

[2] Zhou, Yan (2020): Beidou-3 Global Satellite Navigation system completion and opening ceremony [EB/OL], July 31 2020, http://www.beidou.gov.cn/yw/gfgg/202007/t202 00729_20864.html

[3] Su, Chengeng; Guo, Shuren; Liu, Xunan; et al (2020): Evaluation of Spatial Signal Quality in Beidou-3 Basic System Journal of Electronics and Information, 2020, 42(11):2689-2697.

[4] Yang, Yuanxi; Gao, Weiguang; Guo, Shuren; et al(2019): Introduction to BeiDou-3 navigation satellite system. Navigation, 2019, 66: 7–18.

[5] Zang, Nan; Li, Bofeng; Shen, Yunzhong (2017): Comparison and Analysis PPP 3 GPS BDS Combination Models Journal of Surveying and Mapping 2017, 46(12):1929-1938.

[6] Yan, Li; Li, Meng (2017): BDS GPS Relative Positioning Accuracy Factor Analysis [J].] Journal of surveying and Mapping, 2017, 46(03):325-331.

[7] Wang, Shijin; Bei, Jinzhong; Gu, Shouzhou (2014): BDS/GPS Combination Relative Positioning Method and Precision Analysis [J]. Survey and Mapping Bulletin, 2014(05):1-4.

[8] Jin, Biao; Yang, Shaowen; Liu, Wanke (2013): GPS/BDS Combined Single Point Positioning Algorithm and Analysis of Results [J] and Marine surveying and mapping, 2013, 33(04):39-41 65.

[9] Zhang, Shuhong; Li, Jinlong; Ma, Junfeng (2017); A Preliminary Evaluation of Static Measurement Precision of Beidou Medium-length Base Line Surveying and Mapping Engineering 2017, 26(04):27-3.

[10] Pu, Yakun; Yuan, Yunbin; Ding, Wenwu (2020):Study on the Application of GPS/BDS-2/Galileo Hybrid Double Difference Relative Positioning Model to Precision Positioning of Short Base Line Geodesy and Geodynamics, 2020, 40(01):56-61.

[11] Wu, Mingkui; Liu, Wanke; Zhang, Xiaohong (2020): Preliminary Evaluation of Relative Positioning Performance of Short Base Line Tight Combination of GPS/Galileo/BDS-3 Tests Journal of Wuhan University (Information Science Edition) 2020, 45(01):13-20.

[12] Jin, Jianjian; Gao, Chengfa; Zhang, Ruicheng (200):.Precision Analysis of Short Base Line Resolution for GPS and BDS-2、BDS-3 Fusion Data Survey and Mapping Bulletin, 2020(03): 83-86 95.

[13] Zhang, Baocheng; ou, Jikun; Yuan, Yunbin (2010):Precision Single Point Positioning Algorithm and Application [J] Based on GPS Two-Frequency Original Observations Journal of Surveying and Mapping, 2010, 39(05): 478-483.

[14] Zhang, Xiaohong; Liu, Gen; Guo, Fei (2018): Comparison and Analysis of Positioning Performance of Beidou Three Frequency Precision Single Point Positioning Model [J] and Journal of Wuhan University (Information Science Edition) 2018, 43 (12):2124-2130.

[15] Liu, Tianjun (2019): GPS/Galileo Non-differential Non-combination Real-time Precision Single Point Positioning Fast Convergence and Fuzzy Fixation [D]. China University of Mining and Technology, 2019.

[16] Geng, Jianghui; Meng, Xiaolin; Alan H.Dodson; et al (2010). Integer Ambiguity Resolution in Precise Point Positioning: Method Comparison, Journal of Geodesy, 2010, 84 (9) : 569-581.

[17] Yang, Xu; Xu, Aigong; Qin, Xiaoxi;et al (2017): Single Point Location Analysis of BDS/GPS Pseudo-Speed Distance for elevation Angle Weighting Model [J]; and Journal of Navigation and Positioning 2017, 5(02):72-78+85.

[18] Zhang, Xiaohong; Zuo, Xiang; Li, Pan; et al (2015): BDS/GPS Comparison of Convergence Time and Positioning Precision of Precision Single Point Positioning [J].10 Journal of Surveying and Mapping, 2015, 44(03):250-256.

[19] Ding, Pan; Xi, Ruijie; Xiao, Yugang (2016): Analysis of Performance of Beidou Satellite Navigation System for High Precision

Deformation Monitoring in Northeast China Survey and Mapping Bulletin, 2016(04):33-37.

[20] He, Yilei; Wang, Zhiwen; Wang, Zhong; et al (2018):Analysis of the quality of observational data from the Beidou Global Test Satellite Survey and Mapping Bulletin, 2018(12):1-5.

[21] Zhang Qiang (2018): Low-orbit satellite using GPS and Beidou [D].Wuhan University, 2018.

[22] Dong Zhihua, Chen Junping, Zhou Xuhua (2019): GNSS Discontinuuity Analysis and Evaluation of Precision Track Products, Astronomy Journal, 2019, 60 (05): 45-55.

Authors

Huizhong Zhu is an Associate Professor of School of Surveying and Geographic Science of Liaoning Technical University. He obtained his PhD from Wuhan in 2012. His research is focused on high-precision GNSS positioning and data processing and has authored and coauthored 87 peer-reviewed papers.

Jingfa Zhang is a MEng student of School of Surveying and Geographic Science of Liaoning Technical University. His research is focused on high-precision GNSS positioning and data processing.

Jun Li is a PhD student of School of Surveying and Geographic Science of Liaoning Technical University. His research is focused on high-precision GNSS positioning and data processing

Yangyang Lu is a MEng student of School of Surveying and Science of Liaoning Technical University. His research is focused on high-precision GNSS positioning and data processing